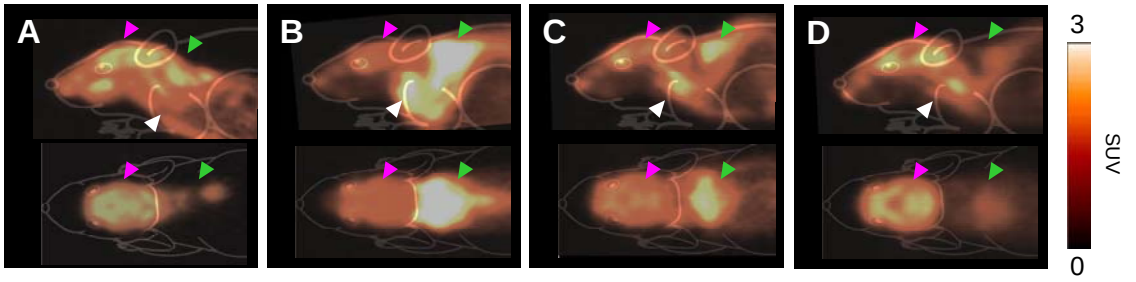

Supplemental Figure 1. PET images with [^{18}F]FDG in conscious mice under four different experimental conditions. Summated images (30–60 min after injection of [^{18}F]FDG) in the sagittal and horizontal planes were acquired under the following conditions: freely moving state as a control (**A**), not warmed or cannulated (**B**), warmed and not cannulated (**C**), and warmed and cannulated (**D**). Arrowheads mark [^{18}F]FDG uptake sites in the brain (pink), brown adipose tissue (green), and skeletal muscle (white).

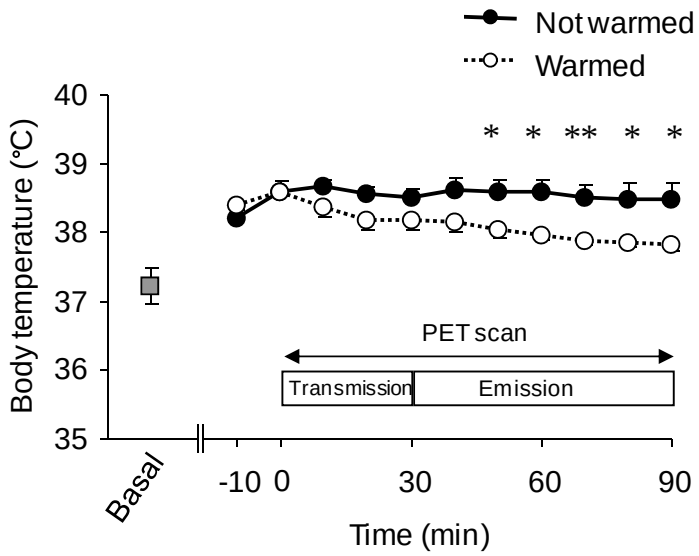

Supplemental Figure 2. Rectal temperature recorded in conscious mice during PET scanning. Change in rectal temperature in conscious mice with or without warming using a temperature controller (closed circles, open circles). Ssquare indicates basal rectal temperature of freely moving mice in their home cage. Error bar, SEM (n = 5); $*P < 0.05$, $**P < 0.01$ indicate differences from the value at the beginning of the PET scan under warmed condition.

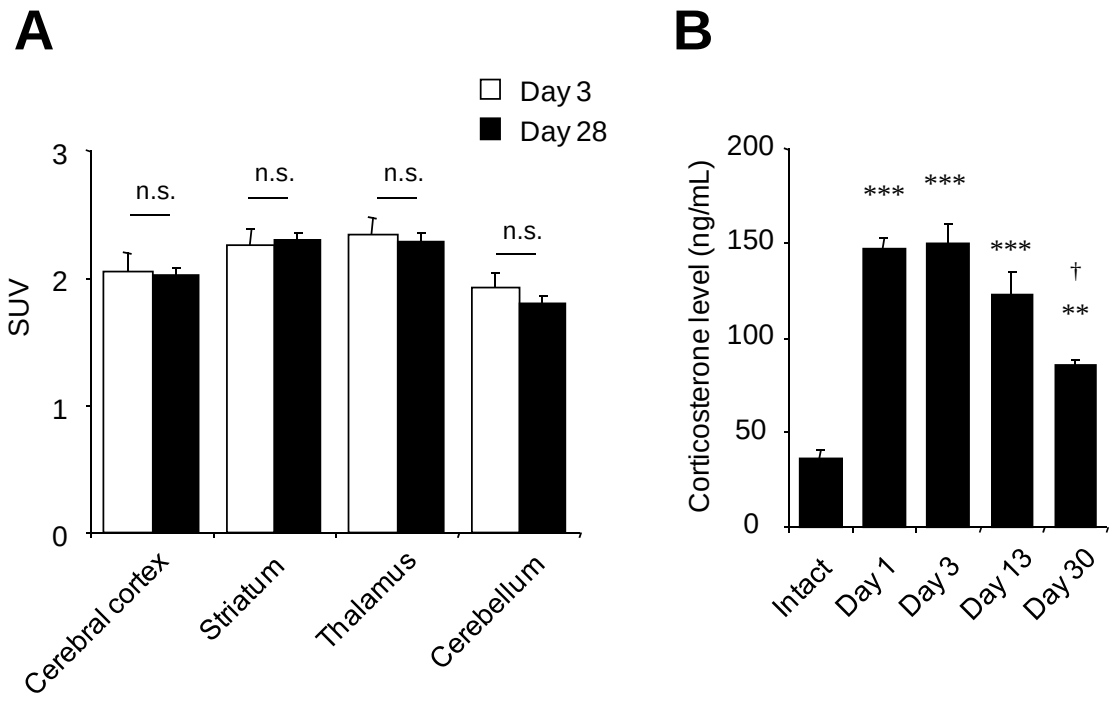

Supplemental Figure 3. Changes in brain [^{18}F]FDG uptake and serum corticosterone levels in conscious mice with head fixation. Comparison of SUV (summated to 30–60 min after injection of [^{18}F]FDG) between 3 and 28 days of acclimation in conscious mice (**A**). Change in serum corticosterone levels (**B**) following acclimation of mice to the immobilizing apparatus for PET scanning under the conscious condition. Error bar, SEM (n = 5); $^{**}P < 0.01$, $^{***}P < 0.001$, vs. intact group; $^{\dagger}P < 0.05$, vs. acclimation to the apparatus on Day 1.

Supplemental Methods

Detection of brain motion for our system of PET scanning of head-fixated mice

Although we successfully obtained PET scans of all of the conscious mice that were immobilized with a custom-made head-fixation system, we used software-based registration to estimate the extent to which the brain had actually moved within a single scan. The list-mode data of the 60-min PET scans were first sorted and reconstructed in 10-framed consecutive dynamic images each consisting of 6 minutes of data. Dynamic images were averaged to form a mean [^{18}F]FDG activity map. A 3D-rectangular volume of interest (VOI) sized 13.9 × 11.1 × 23.9 mm was then placed to cover the whole brain, and this VOI was applied to each of the framed images to extract the part of the image at the same coordinates. Each extracted image was then spatially registered to the mean [^{18}F]FDG map using a 6-parameter rigid body transformation *(1)*. Estimated motion for each framed image was expressed by translation (in millimeters) and rotation (in degrees) for each orthogonal axis: x (left–right), y (rostro–caudal), and z (dorso–ventral). Means and standard deviations of translation and rotation were calculated for each PET scan. As shown in Supplemental Table 1, the estimated size of translation was less than 1 mm in every axis, and that of rotation was less than 2 degrees. Because the spatial resolution of the PET scanner used in the study is greater than 1 mm, we consider that head motion was almost negligible for the PET scanning system used in the present study.

Supplemental references

1) M. Jenkinson, P.R. Bannister, J.M. Brady, and S.M. Smith. Improved optimisation for the robust and accurate linear registration and motion correction of brain images. *NeuroImage*, 17(2):825-841, 2002.

Supplemental Table 1. Estimated head motion during [^{18}F]FDG-PET scanning for each mouse under conscious condition.

	Translation (mm)			Rotation (degree)		
Mouse	X	Y	Z	X	Y	Z
#1	0.27 ± 0.29	0.69 ± 0.74	-0.32 ± 0.39	-1.68 ± 1.89	0.35 ± 0.41	-0.42 ± 0.48
#2	0.16 ± 0.17	0.85 ± 0.92	-0.05 ± 0.09	-1.20 ± 1.43	-0.57 ± 0.62	-0.19 ± 0.22
#3	-0.01 ± 0.11	0.01 ± 0.33	0.00 ± 0.15	-0.04 ± 0.84	-0.02 ± 0.10	0.05 ± 0.16
#4	-0.06 ± 0.07	0.42 ± 0.46	-0.40 ± 0.47	-1.28 ± 1.52	0.24 ± 0.30	0.25 ± 0.28

Data were obtained from 10-framed dynamic images for each PET scan in four animals, and are presented as mean and SD. X, Y, and Z indicate left–right, rostral–caudal, dorsal–ventral axes, respectively.